Nonideal Effects on the Excess Volume from Small to Large Cavities in TIP4P Water

Franca Maria Floris*

Dipartimento di Chimica e Chimica Industriale, Università di Pisa, Via Risorgimento 35, 56126 Pisa, Italy

Received: May 12, 2004; In Final Form: August 3, 2004

Partial molar volumes for hard-sphere cavities in TIP4P water were computed running Monte Carlo simulations in the isothermal, isobaric (NPT) ensemble at 298 K and 1 atm. The explored size range goes from very small cavities up to cavities with a radius of 10 Å. The excess volumes extracted from these data show a nonideal contribution that changes sign for a radius between 8 and 10 Å. The same behavior was also found by computing the quantity directly from distribution functions by means of the Kirkwood−Buff integrals. The results are analyzed also in terms of hydration shell models which are based on the truncation of the Kirkwood−Buff integrals at the distances of the minima of the radial distribution functions. Another choice of truncation based on the oscillatory behavior of the excess volume as a function of the cutoff radius is also considered.

1. Introduction

Many experimental data on partial molar volumes have been collected over the years for a large variety of solutes in different solvents.[1−4] Excess volumes that can be obtained from these data have been analyzed to extract information about solute−solvent and solute−solute interactions in simple solutions and in mixtures.[5,6] The basis of this interpretation is given by the Kirkwood−Buff[7,8] (KB) theory of solutions that links thermodynamic properties to distribution functions. However, this kind of work can be very difficult, especially when applied to complex systems, such as mixtures or biomolecule solutions, because of the overlapping of different solvent effects.[9]

On the contrary, theoretical approaches have not been used very frequently. Integral equation theories have been used to compute the partial molar volumes of ions[10] in water and of simple solutes in hard-sphere or Lennard-Jones systems[11] and to test the group decomposition of amino acid volumes in aqueous solutions.[12] These theories have the advantage of being less expensive than simulations even though a comparison is generally done when possible to test the results. Molecular dynamics and Monte Carlo (MC) simulations have been used in the past decade[13−18] despite the considerable computational effort and some doubts with regard to the use of limited box sizes and closed ensembles. These aspects of the calculation of excess properties using simulations have been treated with a certain effectiveness by Matubayasi et al.[15,19]

However, theoretical approaches can help us to better understand experimental data precisely because we are starting from molecular interactions. Hard-sphere interactions are assumed in simple models[20−23] that can be parametrized to treat hydrophobic solutes in water.[24,25] This kind of interaction is also considered to compute the work of cavity formation included in the decomposition scheme of solvation free energy used in the polarizable continuum model.[26,27] As previously stressed,[27] the choice of the model to describe this term is a very delicate point. Moreover, a model can be parametrized by using different approaches and discrepancies in the parameters can be found. This has been recently shown[28] for the effective hard-sphere diameters extracted from the experimental data of different properties of the simple liquids Ar, Xe, and CH_4. The observed disagreement between different expressions for the cavitation free energy are due to the different assumptions made in their formulation.[28] Nevertheless, such discrepancies do not necessarily indicate the failure of a model. In fact, assumptions are also made by coupling the soft potential used to describe realistic interactions. This is particularly true when extracting cavitation free energies from experimental data.[27,28]

On the contrary, comparison with the simulation results obtained by using hard-sphere potentials would allow a more clear interpretation. We stress that this simple potential is coupled here when introducing the solute cavity in the solvent. This last is instead described by a realistic potential. Extending the comparison to other properties of solutions other than the free energy is a further test of models. Additional information on their performances can be very useful for suggesting improvements or alternative expressions. This study should be seen in this context. Simulation results on the partial molar volumes of cavities of different sizes in TIP4P[29] water are presented. The comparison with simple models is considered, focusing on the nonideal contribution to the excess volumes. Finally, these are analyzed in terms of hydration shell models.[15,19]

2. Method

For a solute (s) in water (w), the partial molar volume is defined as

$$\upsilon_s = \left(\frac{\partial V}{\partial n_s}\right)_{P,T,n_w} \tag{1}$$

with n_s and n_w being the numbers of moles of the solute and solvent, respectively. Using this definition, υ_s was computed from MC simulations in the isothermal, isobaric (NPT) ensemble as the variation in the average volumes ($V(n_s, n_w)$) when the solute is introduced in the solvent

$$\upsilon_s = V(1, n_w) - V(0, n_w) \tag{2}$$

Using the KB theory of solutions in the limit of an infinity dilute solution, υ_s can be computed from the molecular distribution

* Corresponding author. E-mail: floris@dcci.unipi.it.

10.1021/jp047961a CCC: $27.50
Published on Web 09/18/2004

of solvent molecules around the solute, $g_{sw}(\mathbf{x})$, by the equation

$$v_s = kk_BT - \int_0^\infty [g_{sw}(\mathbf{x}) - 1]\, d\mathbf{x} \quad (3)$$

where k_B is the Boltzmann constant, T is the temperature, and k is the isothermal compressibility of the solvent. The second term in the right-hand side of eq 3 is minus the KB integral and defines the excess volume of the solution, namely,

$$\Delta V_{exc} = v_s - kk_BT \quad (4)$$

For a spherical solute, in terms of the radial distribution function (rdf), one has

$$\Delta V_{exc} = -4\pi \int_0^\infty [g_{sw}(r) - 1] r^2\, dr \quad (5)$$

The excess volume can be decomposed in an ideal contribution, that is, the excluded volume, V_0, and a nonideal contribution due to the solute−solvent interactions that determine the solvent reorganization around the solute. For hard-sphere solutes, owing to the shape of the potential, V_0 is simply

$$V_0 = \frac{4}{3}\pi r_{hs}^3 \quad (6)$$

where r_{hs} is the solute−solvent contact distance that defines the cavity radius. As the KB theory has been developed using the grand canonical ensemble, the correlation functions, g_{sw} values, should be computed from simulations in this ensemble. In fact, g_{sw} values derived using different ensembles differ particularly in their asymptotic value, which is exactly 1 only in the grand canonical ensemble. Even if in the other ensembles differences from 1 are very small, on the order of $1/N$ in a closed system,[30,31] their influence on the integral is significant because of the factor r^2 in the integrand. To overcome this problem, one could simply rescale the rdf's computed in a closed system, as Lazaridis[32] proposed.

Moreover, one must take into account that the KB theory cannot be directly applied to the canonical (NVT) ensemble because KB integrals are simply 0 or −1 in this case.[9] As grand canonical simulations are still difficult, even though some progress has been made over the past decade,[33−35] simulations are usually carried out on closed systems. This is one of the reasons for the few applications of the KB theory using rdf's from simulations. However, when using the correct ensemble, other problems still remain that are connected to the limited size of the simulation box that determines the range of the computed rdf. It has been shown[5,36] that the rdf's converge to the asymptotic value only after a distance of several times the diameter of the solvent molecule.

Nevertheless, these problems do not appear serious enough to prevent the application of the KB theory using rdf's from computer simulations.[15−17] In particular, some effort has been made in the works of Matubayasi et al.[15,19] to justify both the use of rdf's from NVT or NPT ensembles and the truncation of the integral. They have shown that an excess property can be decomposed into local and nonlocal components as follows:

$$\Delta Q = \int d\mathbf{x}\, \bar{\rho}(\mathbf{x})[\bar{q}(\mathbf{x}) - \bar{q}_\infty] + \int d\mathbf{x}\, \bar{\rho}(\mathbf{x})(\bar{q}_\infty - q) \quad (7)$$

where $\bar{\rho}(\mathbf{x})$ is the density of the solvent molecules in the solution at position $\mathbf{x}$ and $\bar{q}(\mathbf{x})$ is the local estimator of the property Q. The local component measures the average deviation in the solution of the estimator from its asymptotic value, $\bar{q}_\infty$, while the nonlocal component measures the average contribution from deviations of the asymptotic limit from the value of the estimator in the pure solvent. The interpretation of the second integral in eq 7 as nonlocal is clear because each molecule, wherever its position is in the solution, gives the same contribution. Thus, the first integral is defined as local because the contribution of a molecule depends strongly on its position and in particular molecules very far from the solute do not give any contribution ($\bar{q}(\mathbf{x}) \rightarrow \bar{q}_\infty$).

In the case of the excess volume, the local estimator is $1/\bar{\rho}(\mathbf{x})$, that is, the volume per solvent molecule in the solution.[15] Using eq 7, one has to make different considerations depending on the ensemble. In the grand canonical ensemble, eq 7 reduces to the KB expression (eq 4) as $\bar{\rho}_\infty = \rho_0$ and $\bar{\rho}(\mathbf{x}) = \rho_0 g(\mathbf{x})$. In addition, the excess volume is considered a local property because the second integral is zero. Also, in the NPT ensemble, ΔV is local because $\bar{\rho}_\infty = \rho_0 + O(1/N)$ and the nonlocal contribution is a negligible quantity, as shown by the expression

$$\Delta V_{NPT} = \int d\mathbf{x}\, \bar{\rho}(\mathbf{x})\left[\frac{1}{\bar{\rho}(\mathbf{x})} - \frac{1}{\rho_0}\right] + 0(1) \quad (8)$$

which still reduces to the KB expression if $g(\mathbf{x})$ has been normalized so that $\bar{\rho}(\mathbf{x}) = \rho_0 g(\mathbf{x})$. On the contrary, as mentioned before in the case of the canonical ensemble, the application of eq 7 gives zero because the nonlocal component cancels exactly the local component. The local component defines correctly the excess volume in this ensemble.[19]

Finally, the analysis of the excess property as a function of the cutoff, λ, has shown a damped oscillatory behavior.[15] The hydration shell model proposed by Matubayasi and Levy[15] assumes that the entire contribution to the local component of ΔV comes from the first shell, the other shells giving positive and negative contributions that cancel each other. The validity of the hydration shell model has been proven on the excess volume of methane in TIP4P water.[15] One can better understand the reason for this behavior by analyzing the nonideal contribution to the excess volume ($\Delta V_{ni} = \Delta V_{exc} - V_0$) normalized with respect to the number of solvent molecules in the shell of radius λ:

$$\delta V_{ni}(\lambda) = \frac{\Delta V_{exc}(\lambda) - V_0}{N(\lambda)} = \frac{\Delta V_{exc}(\lambda) - V_0}{\int_0^\lambda d\mathbf{x}\, \bar{\rho}(\mathbf{x})} \quad (9)$$

This quantity represents, in fact, the variation in the average value per solvent molecule in the shell, λ, with respect to the pure solvent, and it must be sensitive to the proximity of the solvent molecules to the solute, whose field is responsible for changes in the solvent distribution. However, in other works,[16,17] the truncation has been made at the cutoff radius imposed by the length of the box used in the simulation. It is clear that the choice of the cutoff is a critical point, as it is relatively arbitrary.

In this work, the solute is a hard-sphere cavity. For this kind of solute in a solvent of hard spheres, partial molar volumes can be evaluated within the scaled particle theory (SPT)[20] or by using the BMCSL equation developed on the basis of a theory of mixtures of hard spheres proposed by Boublik[22] and Mansoori et al.[23] In the following section, the results from NPT simulation by eq 2 are compared to both models applied with an effective hard-sphere diameter for TIP4P water. Moreover, the validity of hydration shell models based on different choices for the truncation radius was checked.

3. Results and Discussion

3.1. v_s from Simulations. Partial molar volumes for hard-sphere cavities in TIP4P water at 298.15 K and 1 atm obtained

TABLE 1: Partial Molar Volumes of Solute Hard Spheres in TIP4P Water from MC Simulations[a]

r_{hs} (Å)	N_w	v_s (cm^3/mol)	r_{hs} (Å)	N_w	v_s (cm^3/mol)
0.95	216	-0.05 ± 0.5	4.05	512	108 ± 3
1.25	216	0.3 ± 0.5	4.45	512	162 ± 3
1.45	216	2.1 ± 0.7	4.70	512	196 ± 2
1.75	216	2.1 ± 0.7	5.05	512	252 ± 2
1.90	216	4.0 ± 0.5	5.45	512	335 ± 2
2.00	216	6.3 ± 0.9	6.05	512	485 ± 3
2.25	216	9 ± 1	6.50	512	629 ± 5
2.55	216	16.0 ± 0.5	7.05	512	826 ± 3
2.85	216	26.2 ± 0.9	7.50	1435	1034 ± 7
3.00	216	33 ± 1	8.00	1435	1276 ± 7
3.20	216	43 ± 2	8.50	1435	1550 ± 8
3.30	216	48 ± 1	9.00	1435	1857 ± 6
3.30	512	47 ± 3	9.50	1435	2222 ± 9
3.45	216	59 ± 1	10.0	1435	2637 ± 7
3.45	512	60 ± 2			

[a] The numbers of configurations used in the averages were between 5×10^9 and 5×10^{10}.

TABLE 2: Some Properties of TIP4P Water Compared to Experimental Data at 298.15 K and 1 atm

	$N_w = 216$[a]	$N_w = 512$[b]	$N_w = 1435$[c]	expt[d]
ρ (g/cm^3)	0.9921 ± 0.0001	0.9975 ± 0.0002	1.0012 ± 0.0001	0.997
	1.002 ± 0.001[e]	1.001 ± 0.001[e]		
$10^6 k$ (atm^{-1})	52.4 ± 0.2	52.1 ± 0.5	48.6 ± 0.5	45.2
	67 ± 13[f]	60 ± 5[e]		
$10^5\alpha$ (deg^{-1})	57.5 ± 0.6	62 ± 1	58 ± 2	25.7
	94[g]	44 ± 8[e]		

[a] 27×10^9 MC configurations. [b] 16×10^9 MC configurations. [c] 20×10^9 MC configurations. [d] See ref 43. [e] See ref 44. [f] See ref 45. [g] See ref 29.

by using eq 2 are shown in Table 1 together with some details of the NPT Monte Carlo (MC) simulations. The size range of the cavities goes from very small cavities up to cavities with a radius of 10 Å. A slightly modified version of the BOSS[37] program was used. Some results of the pure liquid obtained with 216, 512, and 1435 water molecules are shown in Table 2. Water−water interactions were truncated with a cutoff of $L/2$, except for the box with 1435 molecules, for which the same cutoff as that in the box with 512 molecules was used.

With the aim of reducing the errors on v_s and on the nonideal contribution to the excess volume as much as possible, generally very long simulations were run. Statistical errors were evaluated as standard errors in the block averages, after an analysis of variance with the block length to evaluate sampling correlation. Errors are very significant for the very small cavities ($r_{hs} \leq 2$ Å), as expected. However, partial molar volumes increase so rapidly with the cavity's radius (see Figure 1) that the importance of uncertainties is soon reduced. In all cases, the volumes converged within a threshold below the reported statistical errors. No significant size effects were observed in the two cases, $r_{hs} = 3.3$ Å and $r_{hs} = 3.45$ Å, for which the v_s values computed with 216 and 512 molecules differ within statistical uncertainties.

3.2. Comparison with the SPT and BMCSL Models. The results from MC simulations have been compared with the SPT[20,21] and the BMCSL[22,23] equation parametrized on TIP4P water (see Figure 1). The application of both to TIP4P water needs a parametrization to define an effective hard-sphere radius for water.

The SPT was applied with an effective hard-sphere diameter of 2.912 Å determined by comparison with the MC simulations for the cavitation free energy of solute hard spheres in TIP4P water.[24] The expression used needs also the isothermal compressibility, k, and the coefficient of thermal expansion, α, for which values computed for TIP4P water were used (Table 2). For cavity radii smaller than 3.5 Å, the SPT and simulation results are generally in agreement within statistical uncertainties, but for larger cavities, significant discrepancies are observed (1−14%). Using for k and α the experimental values (see Table 2), the SPT results are slightly better for small cavities and slightly worse for $r > 3.5$ Å, where discrepancies are between 7 and 18%. The SPT model appears much more sensitive to the effective hard-sphere diameter of water than to the values of k and α. By using a value of 2.77 Å, the diameter found by Pierotti[21] by extracting the cavitation free energy from experimental data, the SPT model gives worse results even for small cavities.

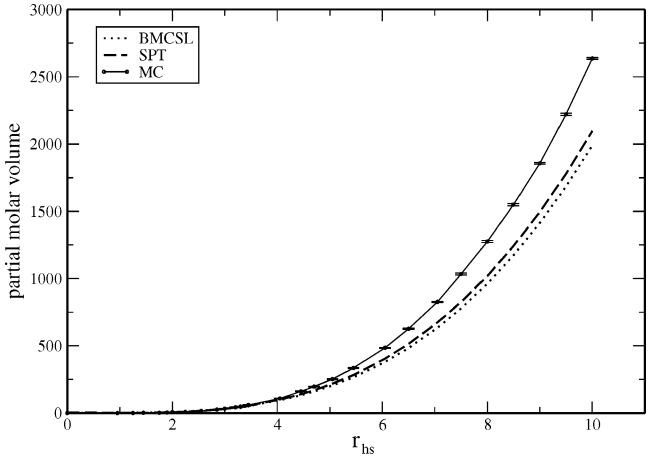

Figure 1. Partial molar volumes, v_s values (cubic centimeters per mole), of hard-sphere cavities in water vs the cavity radius, r_{hs} (angstroms). Comparison of the MC results from eq 2 with respect to the SPT and BMCSL models.

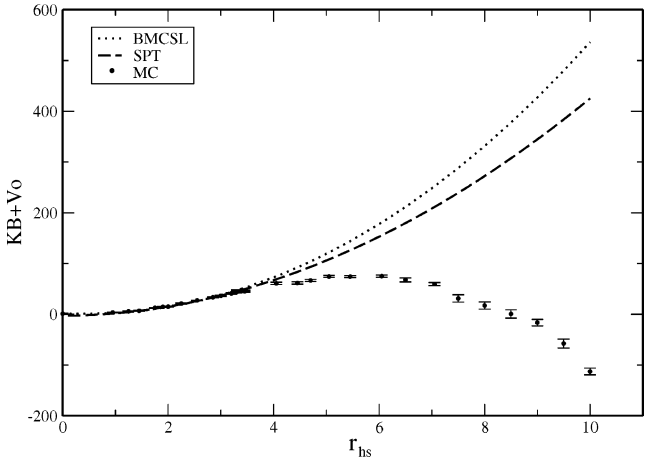

Figure 2. KB + V_0 (cubic centimeters per mole) of hard-sphere cavities in water vs the cavity radius, r_{hs} (angstroms). Comparison of the MC results from eq 2 with respect to the SPT and BMCSL models.

The BMCSL equation for the partial molar volume[38] was applied with an effective diameter for water of 2.564 Å that was determined by comparison of the simulation results with respect to the BMCSL equation for the cavitation free energy in TIP4P water.[25] The results are slightly worse than the SPT model with deviations between 2 and 23%.

To compare more closely the models to the simulation results, KB integrals extracted from the v_s results plus the excluded volumes were plotted in Figure 2. In agreement with what was defined in section 2, this quantity is minus the nonideal contribution to the excess volume ($\Delta V_{ni} = \Delta V_{exc} - V_0$). The

two models are quite similar, with the SPT being generally slightly better than the BMCSL equation except for very small cavities. This could be due to the different range used in fitting the free energies. The BMCSL equation was in fact fitted in the range $r \leq 3.5$ Å, and the SPT was fitted for $r \leq 5.5$ Å.

What is clear is that for both models at ~3.5 Å deviations become systematically positive by increasing the radius of the cavity. In the same region, the discrepancies had been observed to start between the simulation and SPT results for the enthalpic and entropic contributions to the cavitation free energies.[24] Both models always predict a negative nonideal volume in contrast with the simulation results, for which an inversion of the sign is observed between 8 and 10 Å. This means that for cavities with a radius larger than a typical value around 9 Å the nonideal contribution to ΔV_{exc} is positive. This supports the iceberg model of hydrophobic hydration of Frank and Evans[39] only for cavities larger than a particular size. For smaller cavities, the observed volumetric behavior is in contrast with the iceberg model predictions. This has already been noted by Matubayasi and Levy[15] for methane in TIP4P water.

We can explain this behavior by thinking of the plotted quantity as directly connected to the solute−solvent structure in the space accessible to the solvent centers where distribution functions are different from zero. For very big cavities with a radius over a typical value, it can be expected that the structure converges to a limit behavior. As a consequence, the structure contribution to the excess volume in the region accessible to the motion of solvent would converge to a limit value. This must be positive, considering that the limit distribution function can be described as the typical density profile for a liquid−gas interface:[40,41]

$$\rho(r) = \frac{1}{2}\left[\rho_w + \rho_g + (\rho_w - \rho_g)\tanh\left(\frac{r - r_0}{d}\right)\right] \qquad (10)$$

where ρ_w is the density of liquid water and ρ_g the density of water in the gas phase. Here, the latter is zero because of the infinity barrier imposed on the solute−solvent interaction. This expression would be valid also for this kind of interface with only a change of the parameter d that describes its width. Putting $r_0 = r_{hs} + 4.40$ and $d = 1.27$ in the expression above, we found that an infinity limit value of -259 cm^3/mol can be estimated for KB + V_0. The negative sign of this quantity corresponding to a positive nonideal contribution is consistent with the change in sign observed in the simulation results.

3.3. Hydration Shell Models and the Choice of the Truncation Radius. The nonideal contribution to ΔV_{exc} was also computed directly from rdf's. As remarked by Lazaridis,[32] the rdf's from Boss[37] must be renormalized. Otherwise, errors are made that would in particular become significant with an increase of the cavity. In fact, consideration of the whole volume, including the nonaccessible region occupied by the solute, leads to an overestimation of the asymptotic limit value of rdf's. A natural correction might be that of scaling rdf's by $(\langle V\rangle - V_0)/\langle V\rangle$. However, in the same work of Lazaridis,[32] the rdf's computed in the NVT ensemble were scaled by ρ/ρ_0, with $\rho = N_w/V$, while, in another work where rdf's were computed in the NPT ensemble, the rdf's were renormalized, using as the water density the value computed in a region of the solution far from the solute.[16]

Apparently, these different ways of normalization are very similar, but they can produce results that are significantly different. Compare, for example, the four rdf's for the cavity with a radius of $r_{hs} = 3.45$ Å (see Figure 3a) obtained with different boxes and by adopting two different scalings, one based on $\rho^* = N_w/(\langle V\rangle - V_0)$ and the other on ρ_0. The latter was computed coherently with the same number of water molecules used in the box containing the cavity. In this regard, it is important to note that the water density for fixed-charge models[42] has shown only a small dependence on the number of molecules. Although the effect is only around 1% (see also Table 2), this would influence KB integrals significantly, according to what was said before. Looking at the plot of KB + V_0 (see Figure 3b) for a fixed number of molecules as a function of the cutoff, λ, one can see the scaling effect corresponding to densities with differences of around 0.5%.

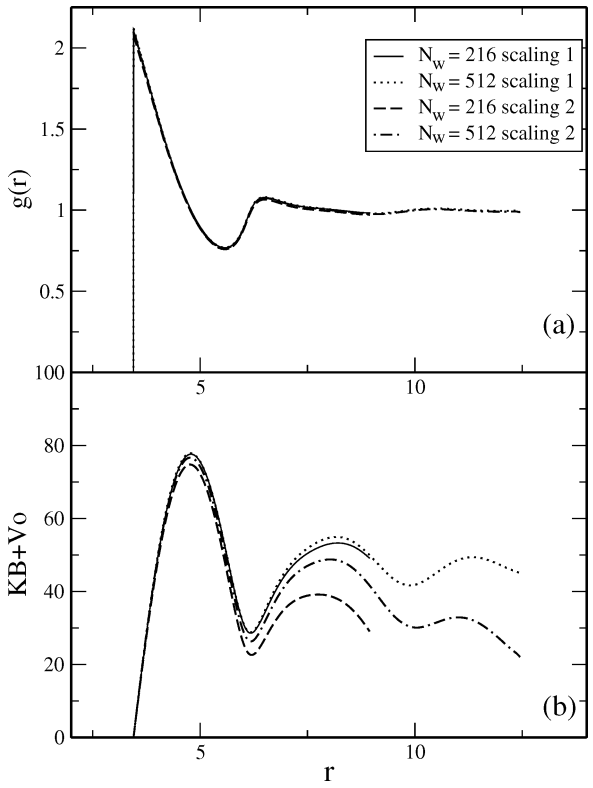

Figure 3. (a) Plot of the radial distribution functions for a hard-sphere cavity with $r_{hs} = 3.45$ Å obtained by MC simulations with different numbers of water molecules, N_w values. The comparison between two different scalings is considered: scaling 1 using the density of pure water and scaling 2 using $\rho^* = N_w/(\langle V\rangle - V_0)$. (b) Plot of KB + V_0 obtained with the rdf's in part a as a function of the truncation radius in the KB integrals. Radius in angstroms and volume in cubic centimeters per mole.

Using the density of the pure solvent coherently determined, one observes a very small effect of box size also at medium range distances. However, this scaling permits the reduction of the correct expression in the NPT ensemble (eq 8), which is independent from the scaling, to the KB expression (eq 5). We can also see that by increasing the distance the small differences in scaling would bring about significant errors in the evaluation of the KB integrals, especially if the truncation is made beyond the first shell. A truncation at the first minimum of the solute−solvent rdf, as in the simplest hydration shell model, is that which least depends on differences in the asymptotic value of the rdf.

As mentioned in section 2 and in agreement with Matubayasi et al,[15,19] this model is capable of capturing the main features of nonideal effects on the excess volume. Its foundations are based on ΔV_{exc} being a local property. This is shown more clearly by the corresponding quantity normalized to the number of molecules in the shell (eq 9). In Figure 4, this quantity has been plotted for some cavities as a function of $\lambda - r_{hs}$. It is

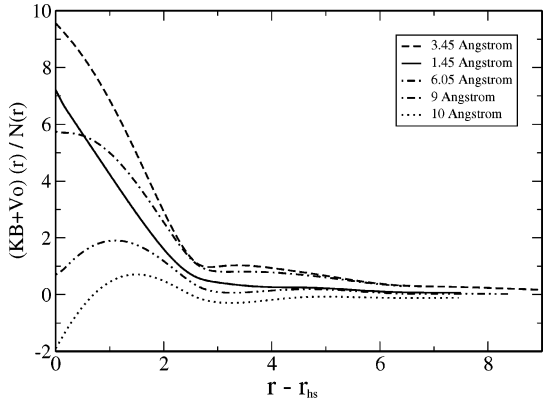

Figure 4. Plot of $-\delta V_{ni}$ (see eq 9) as a function of $r - r_{hs}$ (angstroms) for some cavities of radius r_{hs}. Volumes in cubic centimeters per mole.

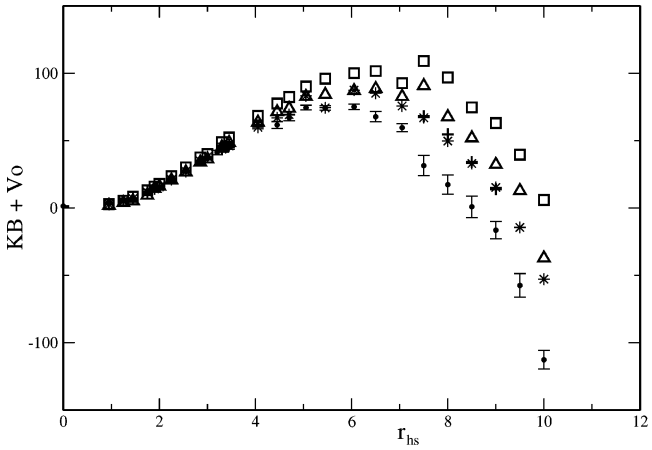

Figure 5. KB + V_0 (cubic centimeters per mole) of hard-sphere cavities in water vs the cavity radius, r_{hs} (angstroms). A comparison of the MC results from eq 2 with respect to the results acquired by the integration of rdf's with truncation radii according to different hydration shell models. The circles with error bars represent the MC results from eq 2; the squares, triangles, and plus signs represent the hydration shell model based on the truncation radius at the first, second, and third minimum of the rdf, respectively; and the stars represent the hydration model based on the truncation at the average radius of radii corresponding to the two last critical points of KB + V_0.

evident by this figure that this property is very sensitive to the distribution of the solvent molecules in close proximity to the cavity surface rather than to the radius of the cavity itself. The quantity is reduced to a very small value for molecules that are three to four molecular diameters away from the cavity surface.

Finally, different hydration shell models were considered on the basis of the truncation at the first, second, and, when possible, the third minimum of the rdf. In addition, a further model, justified by the oscillatory behavior of the integral plotted in Figure 4b, considers for the property KB + V_0 the value at the average between the distances corresponding to the last critical points of the integral. The models are compared with the simulation results obtained directly from υ_s calculations (see Figure 5). All the models give the same trend with the size of the cavity. The agreement is very good for small cavities up to ~4 Å. In this range, also the hydration model based on the first shell could be considered a quite good approximation. For larger cavities, contributions of the second shell improve the results significantly. These agree generally with those of the additional model corresponding to the value around which the oscillations of the integral occur. However, for the larger cavities, deviations with respect to the simulation results from υ_s are over the estimated statistical uncertainties. On one hand, the results

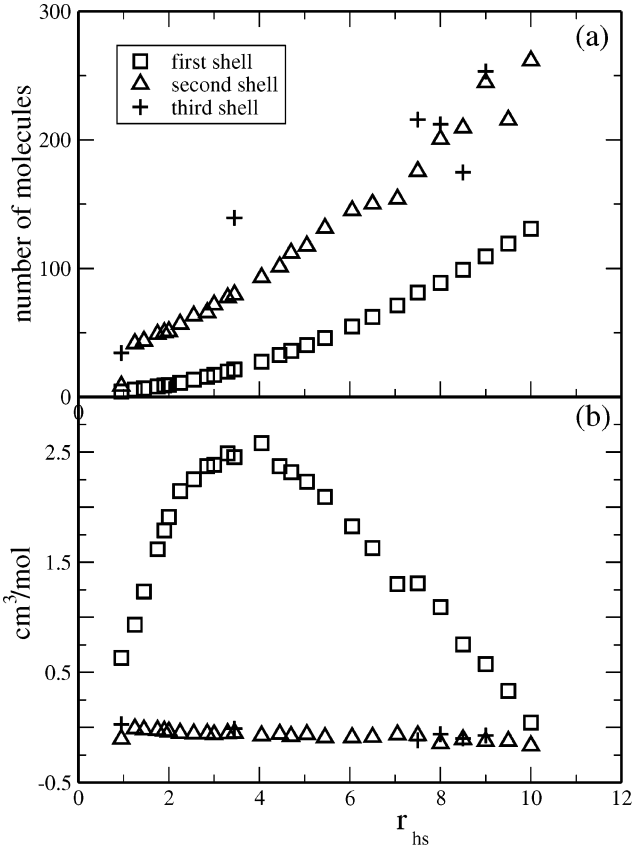

Figure 6. (a) The number of molecules in the first, second, and third hydration shells as a function of the cavity radius. The shells here are usually defined as the region between two spheres. (b) χ_l (see eq 11) in the shells as a function of the cavity radius (angstroms).

obtained with the largest box could be further improved. On the other hand, the discrepancies might be due to the very large number of molecules in the shells beyond the second one.

To better understand the reasons for the observed deviations, it can be useful to write KB + V_0 as a sum over the shells

$$\mathrm{KB} + V_0 = \sum_{l}^{\text{shells}} w_l \chi_l \tag{11}$$

where w_l is the number of molecules in the shell, namely,

$$w_l = N(\lambda_l) - N(\lambda_{l-1}) \tag{12}$$

and χ_l the contribution per molecule averaged on the shell, which according to eq 9 can be written as

$$\chi_l = -\left[\delta V_{ni}(\lambda_l) + \frac{N(\lambda_{l-1})}{w_l}(\delta V_{ni}(\lambda_l) - \delta V_{ni}(\lambda_{l-1}))\right] \tag{13}$$

with $N(\lambda_0) = 0$. The number of molecules in the first three shells and the corresponding values of χ_l are plotted as a function of the cavity radius in Figure 6. It can be seen how χ_1 mainly determines the non-monotonic behavior of KB + V_0 with respect to the cavity radius. The approximate constancy observed between 4 and 6 Å in Figure 5 appears in this context as the result of two contrasting behaviors, the decreasing of χ_1 and the increasing of w_1. The not as good performances, observed for larger cavity radii, of the hydration shell model based on the first minimum of the rdf appear to be related to both, the decreasing of χ_1 and the increasing of the number of molecules in the second shell. The latter is always larger than the number

of molecules in the first shell and is responsible for the increasing importance of the second shell contributions. For a cavity radius of 10 Å, such importance is due not only to a larger value of w_2 but also to a larger value of χ_2 with respect to the corresponding values for the first shell. In addition, molecules belonging to the second shell are determinant for the observed sign inversion of $KB + V_0$, with χ_1 always being positive and χ_2 always being negative. For the larger cavities, also the third shell is important, giving contributions generally comparable to that of the second shell.

4. Conclusions

Nonideal contributions to the excess volumes directly extracted from NPT simulation results of partial molar volumes for hard-sphere cavities in TIP4P water show an interesting behavior versus the cavity radius. An inversion of sign is observed for a cavity radius between 8 and 10 Å. In contrast, the SPT and BMCSL models applied using an effective hard-sphere radius for water predict a monotonic decrease with negative contributions. Discrepancies occur for cavities with a radius larger than 3.5 Å, the same region where the SPT model had shown discrepancies with the simulation results for the enthalpic and entropic contributions to the cavitation free energy.[24] According to the simulation results, the volumetric behavior in the solvation process of a hydrophobic solute is in agreement with the iceberg model[39] only for cavities larger than a particular size. The failure of the iceberg model for cavities with a radius less than $\simeq$9 Å agrees with what Matubayasi and Levy[15] found from NVT simulations for methane in TIP4P water. The inversion of sign of nonideal contributions between 8 and 10 Å was confirmed by the calculation of $KB + V_0$, which relates these quantities to the solute−solvent rdf's. In addition, this behavior is consistent with a positive nonideal contribution which was estimated from the density profile of a planar interface.

The comparison of different hydration shell models with respect to the MC results obtained by eq 2 has shown that the simplest hydration shell model which is based on the first shell is a quite good approximation for a cavity with a radius <4 Å. By increasing the cavity radius, a hydration shell model that includes contributions from molecules in the second hydration shell improves the results significantly. Nevertheless, this is not sufficient to have a quantitative agreement for the larger cavities. It can be supposed that in these cases an accurate hydration shell model needs the inclusion of contributions beyond the third shell. These conclusions are supported by the analysis done in terms of contributions per molecule averaged in the shells.

References and Notes

(1) Millero, F. J. *Chem. Rev.* **1971**, *71*, 1971.
(2) Millero, F. J.; Surdo, A. L.; Shin, C. *J. Phys. Chem.* **1978**, *82*, 784.
(3) Cabani, S.; Gianni, P.; Mollica, V.; Lepori, L. *J. Solution Chem.* **1981**, *10*, 563.
(4) Yasuda, Y.; Tochio, N.; Sakurai, M.; Nitta, K. *J. Chem. Eng. Data* **1998**, *43*, 205.
(5) Matteoli, E., Mansoori, G. A., Eds. *Advances in Thermodynamics Fluctuation Theory of Mixtures*; Taylor & Francis: New York, 1990; Vol. 2.
(6) Matteoli, E. *J. Phys. Chem. B* **1997**, *101*, 9800.
(7) Kirkwood, J.; Buff, F. *J. Chem. Phys.* **1951**, *19*, 774−777.
(8) Newman, K. E. *Chem. Soc. Rev.* **1994**, *23*, 31.
(9) Ben-Naim, A. *Statistical Thermodynamics for Chemists and Biochemists*; Plenum: New York, 1992.
(10) Kusalik, P. G.; Patey, G. N. *J. Chem. Phys.* **1988**, *89*, 5843.
(11) Lazaridis, T. *J. Phys. Chem. B* **1998**, *102*, 3542.
(12) Imai, T.; Kinoshita, M.; Hirata, F. *J. Chem. Phys.* **2000**, *112*, 9469.
(13) Pratt, L.; Pohorille, A. *A. Proc. EBSA Workshop on Water-Biomolecular Interactions* **1992**, *43*, 261.
(14) Paulatis, M. E.; Ashbaugh, H. S.; Garde, S. *Biophys. Chem.* **1994**, *51*, 349.
(15) Matubayasi, N.; Levy, R. M. *J. Phys. Chem. B* **1996**, *100*, 2681.
(16) Lin, C. L.; Wood, R. H. *J. Phys. Chem.* **1996**, *100*, 16399.
(17) Chitra, R.; Smith, P. E. *J. Chem. Phys.* **2001**, *114*, 426.
(18) Lockwood, D. M.; Rossky, P. J. *J. Phys. Chem.* **1999**, *103*, 1982.
(19) Matubayasi, N.; Gallicchio, E.; Levy, R. M. *J. Chem. Phys.* **1998**, *109*, 4864.
(20) Reiss, H.; Frish, H.; Lebowitz, J. *J. Chem. Phys.* **1959**, *31*, 369.
(21) Pierotti, A. *Chem. Rev.* **1976**, *76*, 717.
(22) Boublik, T. *J. Chem. Phys.* **1970**, *53*, 471.
(23) Mansoori, G. A.; Carnhan, N. F.; Starling, K. E.; Leland, T. W. *J. Chem. Phys.* **1971**, *54*, 1523.
(24) Floris, F.; Selmi, M.; Tani, A.; Tomasi, J. *J. Chem. Phys.* **1997**, *107*, 6353.
(25) de Souza, L. E. S.; Ben-Amotz, D. *J. Chem. Phys.* **1994**, *101*, 9858.
(26) Amovilli, C.; Barone, V.; Cammi, R.; Cancès, E.; Cossi, M.; Mennucci, B.; Pomelli, C. S.; Tomasi, J. *Adv. Quantum Chem.* **1999**, *32*, 227.
(27) Amovilli, C.; Floris, F. M. *Phys. Chem. Chem. Phys.* **2003**, *5*, 363.
(28) Nasehzadeh, A.; Azizi, K. *THEOCHEM* **2003**, *638*, 197.
(29) Jorgensen, W.; Chandrasekhar, J.; Madura, J.; Impey, R.; Klein, M. *J. Chem. Phys.* **1983**, *79*, 926.
(30) Hill, T. *Statistical Mechanics*; Dover Publications: New York, 1956.
(31) Lebowitz, J. L.; Percus, J. K. *Phys. Rev.* **1961**, *122*, 1675.
(32) Lazaridis, T. *J. Phys. Chem. B* **1998**, *102*, 3531.
(33) Beutler, T. C.; Mark, A. E.; van Schaik, R. C.; Gerber, P. R.; van Gunsteren, W. F. *Chem. Phys. Lett.* **1994**, *222*, 529.
(34) Zacharias, M.; Straatsma, T. P.; McCammon, J. *J. Chem. Phys.* **1994**, *100*, 9025.
(35) Weerasinghe, S.; Pettitt, B. M. *Mol. Phys.* **1994**, *82*, 897.
(36) Shulgin, I.; Ruckenstein, E. *J. Phys. Chem. B* **1999**, *103*, 4900.
(37) Jorgensen, W. *BOSS*, version 3.5; Yale University Press: New Haven, CT, 1994.
(38) Ben-Amotz, D. *J. Phys. Chem.* **1993**, *97*, 2314.
(39) Frank, H. S.; Evans, M. W. *J. Chem. Phys.* **1945**, *13*, 507.
(40) Matsumoto, M.; Kataoka, Y. *J. Chem. Phys.* **1988**, *88*, 3233.
(41) Huang, D.; Chandler, D. *J. Phys. Chem. B* **2002**, *106*, 2047−2053.
(42) Mahoney, M. W.; Jorgensen, W. L. *J. Chem. Phys.* **2000**, *112*, 8910.
(43) Kell, G. *J. Chem. Eng. Data* **1975**, *20*, 97.
(44) Jorgensen, W.; Jensen, C. *J. Comput. Chem.* **1998**, *19*, 1179.
(45) Jorgensen, W.; Madura, J. *Mol. Phys.* **1985**, *56*, 1381.